Mechanism of Specific Target Recognition and RNA Hydrolysis by Ribonucleolytic Toxin Restrictocin†

Surendra K. Nayak,‡,§ Shveta Bagga,‡,§ Deepak Gaur,‡,§ Deepak T. Nair,|| Dinakar M. Salunke,|| and Janendra K. Batra*,‡

Immunochemistry Laboratory and Structural Biology Unit, National Institute of Immunology, Aruna Asaf Ali Road, New Delhi 110067, India

Received May 7, 2001; Revised Manuscript Received June 7, 2001

ABSTRACT: Restrictocin, a member of the fungal ribotoxin family, specifically cleaves a single phosphodiester bond in the 28S rRNA and potently inhibits eukaryotic protein synthesis. Residues Tyr47, His49, Glu95, Phe96, Pro97, Arg120, and His136 have been predicted to form the active site of restrictocin. In this study, we have individually mutated these amino acids to alanine to probe their role in restrictocin structure and function. The role of Tyr47, His49, Arg120, and His136 was further investigated by making additional mutants. Mutating Arg120 or His136 to alanine or the other amino acids rendered the toxin completely inactive, whereas mutating Glu95 to alanine only partially inactivated the toxin. Mutation of Phe96 and Pro97 to Ala had no effect on the activity of restrictocin. The Tyr47 to alanine mutant was inactive in inhibiting protein synthesis, and had a nonspecific ribonuclease activity on 28S rRNA similar to that shown previously for the His49 to Ala mutant. Unlike the His136 to Ala mutant, the double mutants containing Tyr47 or His49 mutated to alanine along with His136 did not compete with restrictocin to cause a significant reduction in the extent of cleavage of 28S rRNA. In a model of restrictocin and a 29-mer RNA substrate complex, residues Tyr47, His49, Glu95, Arg120, and His136 were found to be near the cleavage site on RNA. It is proposed that in restrictocin Glu95 and His136 are directly involved in catalysis, Arg120 is involved in the stabilization of the enzyme−substrate complex, Tyr47 provides structural stability to the active site, and His49 determines the substrate specificity.

Restrictocin, produced by the fungus *Aspergillus restrictus*, is a nonglycosylated, single-chain, basic protein containing 149 amino acids (*1*). Restrictocin and two other known members, α-sarcin and mitogillin produced by different *Aspergillus* species, constitute a group of toxins called ribotoxins (*2*). Ribotoxins are extremely potent inhibitors of eukaryotic protein synthesis (*3*). They act as highly specific ribonucleases by cleaving a single phosphodiester bond between G4325 and A4326 in a 12-nucleotide purine-rich universally conserved stem and loop domain in the 28S rRNA termed the sarcin domain which is critical for the ribosome function (*4*, *5*). Cleavage of 28S rRNA by ribotoxins produces a fragment ∼400 nucleotides in length, which has been termed the α-fragment (*4*). The specific cleavage of rRNA by ribotoxins impairs the EF-1-dependent binding of aminoacyl tRNA and GTP-dependent binding of EF-2 to ribosomes, which in turn leads to a total collapse of the translational machinery, resulting in cell death (*3*, *6*). Using several variants of a 35-mer and a 29-mer synthetic oligoribonucleotide that mimic the conserved nucleotides and the secondary structure of the sarcin domain of ribosomal RNA, it is shown that to retain substrate specificity, a stem containing a minimum of three base pairs and a guanine base six bases 5′ to the cleavage site were essential (*7*−*9*). The crystal structure of the 29-mer nucleotide RNA containing the sarcin loop has been reported recently (*10*).

The X-ray crystal structure of restrictocin reveals that the structural core consists of a five-stranded antiparallel β-sheet stabilized by a three-turn α-helix in a perpendicular position. Another long, two-stranded antiparallel β-sheet is located at the N-terminus (*11*). There are large connecting loops between the β-strands. The curved β-strands are highly twisted in a right-handed manner and form a shallow cleft which presumably forms the active site of the toxin (*11*). The sequence of restrictocin is 22 and 24% identical to the sequences of RNase T1 from the fungus *Aspergillus oryzae* and RNase U2 from *Ustilago sphaerogena*, respectively (*1*, *12*). While RNases T1 and U2 cleave RNA after every guanine base, only fungal ribotoxins demonstrate specific cleavage of a single phosphodiester bond in 28S rRNA in the large ribosomal subunit. The structure of the core in restrictocin closely resembles that in RNase T1, suggesting that they have similar catalytic mechanisms (*11*).

On the basis of structural analysis, predictive studies, and sequence homology with other ribonucleases, it has been proposed that Tyr47, His49, Glu95, Phe96, Pro97, Arg120,

† This work was supported by grants to the National Institute of Immunology from the Department of Biotechnology, Government of India. S.K.N. is a Senior Research Fellow of the National Institute of Immunology. S.B., D.G., and D.T.N. thank the Council of Scientific and Industrial Research, India, for senior research fellowships.

* To whom correspondence should be addressed. Phone: 91-11-6163009/6162281. Fax: 91-11-6162125/6109433. E-mail: janendra@nii.res.in.

‡ Immunochemistry Laboratory.

§ These authors contributed equally to this work.

|| Structural Biology Unit.

10.1021/bi010923m CCC: $20.00
Published on Web 07/10/2001

Table 1: Sequence of Primers Used for Mutagenesis of the Putative Active Site Residues[a]

mutant	primer	sequence
Y47A	SY47A	5′ AACCAGTGCGGGgcGCTGgatCCGGTCTTGCCGTC 3′
E95A	SK10	5′ TCGGGAAtgctAGCAGGT 3′
F96A	SF96A	5′ GGAAAAGTCGGGgcCTCgAGCAGGTAGTGGTCATC 3′
P97A	SP97A	5′ GGAAAAGTCGcGAACTCgAGCAGGTAGTGGTCATC 3′
R120A	SR120A	5′ ATAAGTATAGATGACtgcaGCTGGGCCCGGGTCTT 3′
R120Q	JKB 69	5′ ATAAGTATAGATGACctgCGCTGGGCCCGGGTCTT 3′
R120K	JKB 70	5′ ATAAGTATAGATGACcttCGCTGGGCCCGGGTCTT 3′
R120H	JKB 71	5′ ATAAGTATAGATGACgtgCGCTGGGCCCGGGTCTT 3′
H136A	SH136A	5′ TGATTCCCCCGCTGCgcaGCCACAATGCCGCAAAA 3′
H136R	JKB 66	5′ CTGATTCCCCCGCTGcctGGCCACAATGCCGCAAA 3′
H136N	JKB 67	5′ CTGATTCCCCCGCTGgttGGCCACAATGCCGCAAA 3′
H136D	JKB 68	5′ CTGATTCCCCCGCTGgtcGGCCACAATGCCGCAAA 3′

[a] The lowercase letters represent the mutated nucleotides, and the underlined sequence denotes the restriction sites created in the primer. The restriction sites were created to facilitate screening of the mutants.

and His136 form the active site of restrictocin (*11*, *12*). Mutation of His136 in restrictocin and the corresponding residue His137 in α-sarcin has been shown to inactivate the toxins (*13*, *14*). Glu95 seems to play a less critical role as mutation of this residue to glycine is shown to partially inactivate restrictocin (*13*). We have previously shown that with the mutation of His49 to alanine, the specific substrate recognition activity of restrictocin is abolished (*15*). Kao et al. (*16*) have shown, by chemical mutagenesis, that His49, Glu95, Arg120, and His136 are important for catalysis in mitogillin. Restrictocin contains four cysteine residues involved in two disulfide bonds. We have shown recently that none of the four cysteines is directly involved in restrictocin catalysis, and either one of the two disulfides is enough to provide the functional conformation to the protein (*17*). The ribotoxins have great potential to be utilized for the construction of immunotoxins. Immunotoxins and chimeric toxins with potent activity on various tumor cell lines have been made with restrictocin (*18*−*21*). Detailed information about the essential residues would help in further engineering the toxin molecule.

In this study, to investigate the precise role of the residues predicted in the active site of restrictocin, Tyr47, His49, Glu95, Phe96, Pro97, Arg120, and His136 have been mutated to alanine and Arg120 and His136 to several other amino acids. The mutants were expressed in *Escherichia coli* and purified to homogeneity. The study shows that Glu95, Arg120, and His136 are absolutely essential for the RNA cleavage by restrictocin whereas Tyr47 and His49 are involved in the specific recognition of the target RNA by the protein, and Phe96 and Pro97 are not involved in the functional activity of restrictocin.

EXPERIMENTAL PROCEDURES

Construction of Restrictocin Mutants. Restrictocin has been overexpressed in *E. coli* and purified from the inclusion bodies to obtain the functionally active toxin (*22*). The plasmid pRest, containing the restrictocin gene cloned downstream of the T7 promoter, was used as the template to mutate amino acid residues Tyr47, Glu95, Phe96, Pro97, Arg120, and His136 to alanine by oligonucleotide-mediated mutagenesis (*23*). In addition, Arg120 was mutated to glutamine, lysine, and histidine, and His136 was mutated to arginine, asparagine, and aspartic acid. The uracil-containing DNA template was prepared by infecting the CJ236 strain of *E. coli* with the recombinant phage and growing it in the presence of uridine and chloramphenicol. Mutagenesis was performed using DNA primers SY47A, SK10, SF96A, SP97A, SR120A, JKB69, JKB70, JKB71, SH136A, JKB66, JKB67, and JKB69 containing the Tyr47Ala, Glu95Ala, Phe96Ala, Pro97Ala, Arg120Ala, Arg120Gln, Arg120Lys, Arg120His, His136Ala, His136Arg, His136Asn, and His136Asp mutations, respectively. The list of the various primers used along with their sequence is given in Table 1. Primer extension products were transformed into *E. coli* strain DH5α by standard methods. The H49A mutant was constructed by sequential polymerase chain reaction (PCR)[1] as described previously (*15*). For the construction of the H49A/H136A double mutant, the H49A single mutant was used as the template for creating the second mutation by oligonucleotide-mediated mutagenesis using the SH136A primer (*23*). To construct the Y47A/H136A mutant, mutants Y47A and H136A were digested with *Hin*dIII (a *Hin*dIII restriction site was created at position 178 in the restrictocin gene) and *Eco*RI (present at the 3′ end of restrictocin), and the fragment containing the H136A mutation was ligated with the fragment containing the Y47A mutation. The mutations were confirmed by DNA sequencing using the dideoxy chain termination method (*24*).

Expression and Purification of Recombinant Proteins. Restrictocin and its mutants were expressed in the BL21-(λDE3) strain of *E. coli*. Bacterial cells, transformed with the appropriate plasmids, were grown in super broth at 37 °C with vigorous shaking. At an OD_{600} of 2.0, cultures were induced with 1 mM IPTG and grown for a further 2 h. Like restrictocin, all its mutants accumulated in inclusion bodies (*22*), from which the proteins were purified following the procedure described by Buchner et al. (*25*). The purified inclusion bodies were subjected to denaturation in guanidine hydrochloride, reduction by dithioerythritol, and renaturation in a buffer containing arginine and oxidized glutathione. The renatured proteins were dialyzed and purified by successive cation-exchange (S-Sepharose) and gel-filtration (TSK 3000) chromatography as described previously for recombinant restrictocin (*22*).

Characterization of Proteins by Circular Dichroism. CD spectral analysis of restrictocin and its mutants was carried

[1] Abbreviations: CD, circular dichroism; IPTG, isopropyl β-D-thiogalactopyranoside; MRE, mean residue ellipticity; PCR, polymerase chain reaction; SDS−PAGE, sodium dodecyl sulfate−polyacrylamide gel electrophoresis.

out as described previously (*26*). Proteins were dissolved in 10 mM sodium phosphate buffer (pH 7.0), and their CD spectra were recorded on a JASCO J710 spectropolarimeter in the far-UV range at 25 °C. A cell with a 1 cm optical path was used to obtain spectra at a scan speed of 50 nm/min with 50 mdeg sensitivity and a response time of 1 s. The spectra were averaged over 10 accumulations, and the results are presented as the mean residue ellipticity.

Effect of Mutations on in Vitro Protein Synthesis. Rabbit reticulocyte lysate was used to assay the activity of restrictocin and its mutants by investigating their effect on in vitro protein synthesis. Reticulocyte lysate was prepared from rabbit blood, and the assay was carried out as previously described (*15*). The lysate was incubated with different concentrations of various proteins, and incorporation of [^{3}H]-leucine was quantitated in the newly synthesized proteins. Activity was expressed as a percent of control, where no toxin was added. The amount of toxin needed to cause 50% inhibition was termed the ID_{50} value.

Cytotoxic Activity of Restrictocin and Its Mutants. To assess the cytotoxic activity of restrictocin and its mutants, HeLa cells permeabilized by adenovirus infection were used as described previously (*27*, *28*). HeLa cells, grown at a density of 2×10^4 cells per well in 96-well culture plates for 12 h at 37 °C, were incubated with virus and different concentrations of the toxin or mutants at 37 °C for 5 h. Cells were labeled with 0.1 μCi of [^{3}H]leucine per well for an additional 2 h, followed by harvesting and counting on filtermats using an LKB β-plate counter.

Assay of Specific Ribonucleolytic Activity of Restrictocin and Its Mutants. Restrictocin and its mutants were assayed for their specific ribonucleolytic activity using rabbit reticulocyte lysate as the source of 28S rRNA as described previously (*29*). Rabbit reticulocyte lysate was treated with various proteins in 40 mM Tris-HCl (pH 7.5) containing 10 mM EDTA for 15 min at 37 °C. The reaction was stopped by the addition of 0.4% SDS, and total RNA was extracted using Trizol (GIBCO-BRL Life Technologies) solution. RNA was dissolved in 0.5% SDS, electrophoresed on a 1.5% agarose gel, and visualized by ethidium bromide staining.

Activity Staining Assay. Zymogram electrophoresis was carried out as described by Blank et al. (*30*). Various proteins (250 ng each) were subjected to SDS−PAGE under nonreducing conditions on 15% gels containing 0.3 mg/mL RNA substrate. After removing SDS by washing in 2-propanol, we incubated the gel at 37 °C for 1 h and stained it with 0.2% toluidine blue. RNase activity was indicated by the appearance of clear zones on a blue background.

Competition Assay for Specific Ribonuclease Activity of Restrictocin. The ability of mutants H136A, H49A/H136A, and Y47A/H136A to compete with restrictocin to bind to the substrate was studied by preincubating rabbit reticulocyte lysate with the competitor for 30 min on ice in 40 mM Tris-HCl (pH 7.5) containing 10 mM EDTA. At the end of the preincubation, restrictocin was added and the mixture was incubated for 15 min at 37 °C. BSA was used as a nonspecific competitor. The generation of the α-fragment was visualized as described above.

Modeling of the Restrictocin−Substrate Complex. The docking of a 29-mer fragment of natural rRNA substrate into the active site of restrictocin was carried out using the crystal structure of restrictocin, and that of the substrate available in the PDB (*10*, *11*). The PDB accession numbers for restrictocin and the 29-mer substrate are 1AQZ and 430D, respectively. All available RNase T1−substrate complex structures were aligned using the HOMOLOGY module of INSIGHTII. It was seen that the different ligands bind to more or less the same region on the RNase molecule. The restrictocin structure was superimposed onto this alignment of RNase T1−substrate complexes. This superimposition was carried out on the basis of secondary structural elements. The rRNA substrate was picked up and was docked onto the restrictocin molecule in such a way that the cleavage site was present in the region analogous to the region where the various ligands are present on the RNase T1 enzyme. The docking was improved manually to achieve the best possible fit with respect to the intermolecular energy measured using the DOCKING module of INSIGHTII. This was followed by energy-based refinement of the complex in which the conformations of both the RNA substrate and the enzyme were kept flexible. The distance-dependent dielectric constant was used during these calculations. Initially, conjugate gradient energy minimization was carried out till convergence to remove those steric clashes which manual docking did not eliminate. The complex was subjected to molecular dynamics simulation for 200 ps (time step of 1 fs) at 300 K after the system was allowed to equilibrate at the target temperature for 40 000 steps. During the simulation, conformations were written out every picosecond. These conformations were then analyzed using the DECIPHER module in MSI software. Among the conformations that were written out, every tenth conformation was subjected to conjugate gradient minimization till convergence. This set of minimized conformations had intermolecular energies between those of the substrate and enzyme within a range of 15 kcal/mol. The conformation, which exhibited a maximum intermolecular energy (−239 kcal/mol) among these, was selected for comparison with the native restrictocin crystal structure. The contacts formed between the rRNA and restrictocin were determined for all the conformations using the CONTACT program of the CCP4 suite. The changes in the structure of restrictocin on binding to rRNA were measured by calculating the root-mean-square deviation using the positions of all atoms and using Cα atoms only.

RESULTS

Construction of Restrictocin Mutants. To investigate the importance of the residues predicted to be forming the active site of restrictocin, they were mutated to alanine by oligonucleotide-mediated mutagenesis. The various mutants thus constructed included Y47A, H49A, E95A, F96A, P97A, R120A, and H136A. Restrictocin mutants were also made where Arg120 was mutated to Gln, Lys, and His and His136 to Arg, Asn, and Asp. To gain further insight into the role of Tyr47 and His49, two double mutants were constructed where along with His136 either Tyr47 or His49 was mutated to Ala to give rise to the Y47A/H136A and H49A/H136A mutants, respectively. All residues were replaced with alanine to eliminate the side chains beyond the β-carbon without altering the main conformation. All mutations were confirmed by DNA sequencing.

Expression, Purification, and Structural Characterization. The mutants were expressed in the BL21(λDE3) strain of

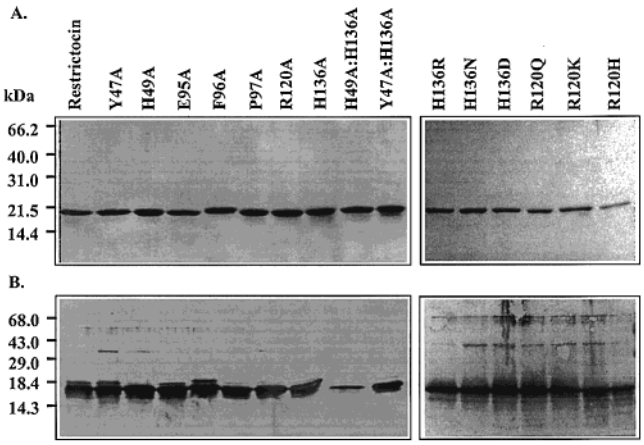

FIGURE 1: SDS−PAGE and Western blot analysis of restrictocin mutants. The mutants were expressed in BL21(λDE3) cells of *E. coli* and purified from inclusion bodies by cation-exchange and gel-filtration chromatography. The recombinant proteins were analyzed by 12.5% SDS−PAGE under reducing conditions followed by Coomassie blue staining (A). Western blot analysis of the mutants was carried out using a polyclonal antibody raised against restrictocin (B). The lanes in panel B correspond to same proteins as in panel A.

E. coli, and were localized in the inclusion bodies such as restrictocin from which they were isolated and purified to homogeneity using conventional chromatography. When analyzed by SDS−PAGE, the mutants gave single bands at the same position as restrictocin, indicating that the preparations were homogeneous (Figure 1A). On Western blots, all the mutants and the native toxin reacted equally well with a polyclonal antibody raised against restrictocin (Figure 1B).

The effect of respective mutations on the overall structure of restrictocin was studied by CD spectral analysis of the purified mutants in the far-UV region. The native restrictocin is an α+β protein with relatively higher β-sheet content. The CD profile of the native protein, therefore, corresponds to the broad minima over the 208−222 nm range, consistent with the structural composition of the protein. The far-UV CD spectra of E95A, F96A, and P97A did not show major changes in the mean residue molar ellipticity of the mutants as compared to that of the native toxin over this wavelength range (Figure 2A). Differences in the amplitudes of the profiles could be attributed to insignificant changes in the α-helix and β-sheet content of the mutants compared to the native toxin. Thus, point mutations E95A, F96A, and P97A did not significantly alter the structure of restrictocin. The CD spectra of H49A, R120A, H136A, and H49A/H136A in the far-UV region were indistinguishable from the CD spectrum of restrictocin, indicating that these mutants had a structure that closely resembled that of the native toxin (Figure 2B). An alteration compared to that of restrictocin was observed in the molar ellipticity curve of the Y47A mutant. The amplitude of the negative peak signal at 218 nm was found to be substantially reduced, implying a loss of β-sheet content of the Y47A mutant compared to the native toxin (Figure 2C). It is relevant to note that Tyr47 is close to strand β3 of the β-sheet that provides a scaffold for the substrate-binding pocket. A similar and more significant structural change was observed in the Y47A/H136A double mutant (Figure 2C). The CD spectra of R120Q, R120K, and R120H were very similar to those of R120A and restrictocin (Figure 2D). The CD spectra of H136N and H136D were also very similar to those of H136A and restrictocin; however, there was a modest alteration in the CD spectrum of H136R (Figure 2E).

Effect of Restrictocin and Its Mutants on in Vitro Protein Synthesis. The ability of restrictocin mutants to inhibit protein synthesis was tested in a rabbit reticulocyte lysate-based cell-

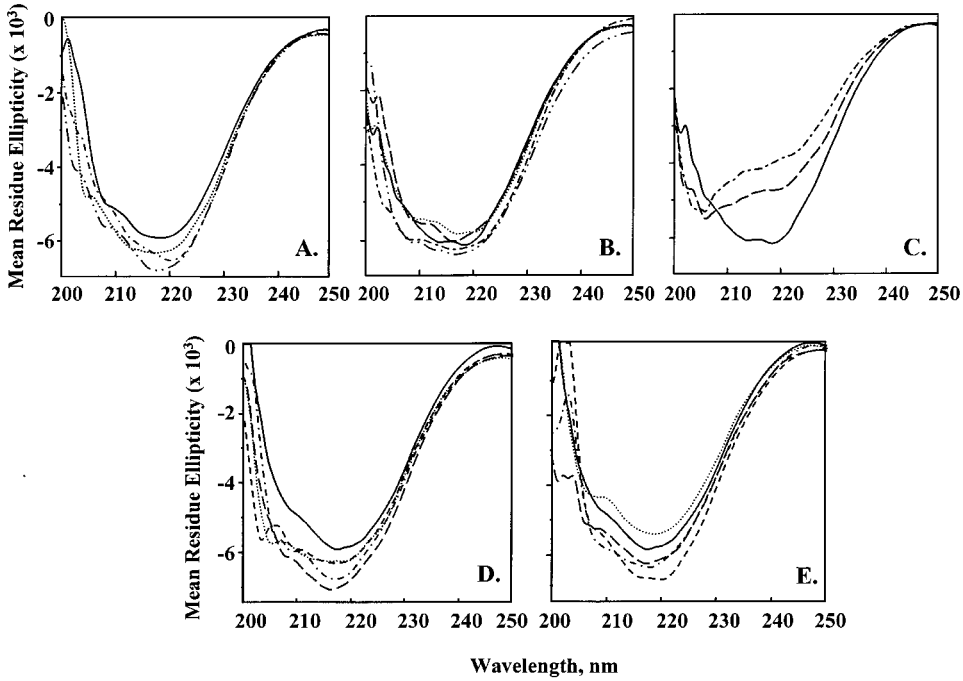

FIGURE 2: CD spectral analysis of restrictocin mutants. CD spectra were recorded in far-UV region (200−250 nm) at 25 °C. The spectra are presented as mean residue ellipticity, expressed in degrees per square centimeter per decimole (×10^{-3}): (A) restrictocin (—), E95A (···), F96A (—··—), and P97A (—·—); (B) H49A (— — —), H136A (···), H49A/H136A (—·—), R120A (—··—), and restrictocin (—); (C) Y47A (— — —), Y47A/H136A (—·—), and restrictocin (—); (D) restrictocin (—), R120A (—·—), R120H (···) R120K (- - -), and R120Q (— — —); and (E) H136A (— — —), H136R (···), H136N (- - -), H136D (—·—), and restrictocin (—).

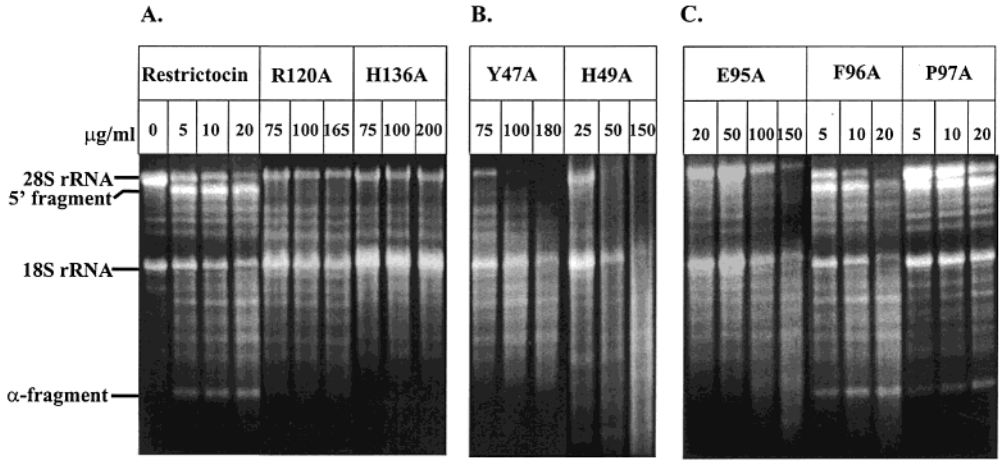

FIGURE 3: Ribonucleolytic activity of restrictocin mutants on 28S rRNA. Rabbit reticulocyte lysate was treated with various concentrations of restrictocin and its mutants as indicated in the figure. Total RNA was extracted and resolved on an agarose gel.

Table 2: Activity of Restrictocin Mutants on in Vitro Protein Synthesis[a]

protein	ID_{50} (ng/mL)	activity
restrictocin	4.4	active
Y47A	250	inactive
H49A	>1000	inactive
E95A	58	partially active
F96A	4.7	active
P97A	5.6	active
R120A	>1000	inactive
R120Q	>1000	inactive
R120K	>1000	inactive
R120H	>1000	inactive
H136A	>1000	inactive
H136R	>1000	inactive
H136N	>1000	inactive
H136D	>1000	inactive
H49A/H136A	>1000	inactive
Y47A/H136A	>1000	inactive

[a] Rabbit reticulocyte lysate was treated with various concentrations of restrictocin mutants at 30 °C for 1 h. Levels of incorporation of [^{3}H]leucine into the newly synthesized polypeptides were measured. ID_{50} refers to the amount of toxin required to inhibit protein synthesis by 50%.

Table 3: Cytotoxicity of Restrictocin Mutants in Adenovirus-Infected HeLa Cells[a]

protein	ID_{50} (μg/mL)	activity
restrictocin	0.17	active
Y47A	>100	inactive
H49A	>100	inactive
E95A	54	partially active
F96A	3.4	partially active
P97A	3.7	partially active
R120A	>100	inactive
H136A	>100	inactive
H49A/H136A	>100	inactive
Y47A/H136A	>100	inactive

[a] HeLa cells were infected with adenovirus and treated with different concentrations of the toxin and mutants. Levels of incorporation of [^{3}H]leucine into the newly synthesized proteins were measured. ID_{50} refers to the amount of toxin required to inhibit protein synthesis by 50%.

free in vitro translation assay. The decrease in the level of incorporation of [^{3}H]leucine in the nascent peptides was taken as the measure of protein synthesis inhibition by the toxin. The native toxin and mutants F96A and P97A potently inhibited protein synthesis in a dose-dependent manner with ID_{50}s of 4.4, 4.7, and 5.6 ng/mL, respectively (Table 2). Though the E95A and Y47A mutants also caused a dose-dependent inhibition of protein synthesis, they were only partially active compared to restrictocin in the assay with ID_{50} values of 58 and 250 ng/mL, respectively, compared to that of 4.4 ng/mL for restrictocin (Table 2). Mutants H49A, R120A, and H136A and double mutants Y47A/H136A and H49A/H136A did not produce any protein synthesis inhibition even up to 1000 ng/mL in this assay (Table 2). Like the R120A and H136A mutants, R120Q, R120K, R120H, H136R, H136N, and H136D also did not produce any protein synthesis inhibition up to 1000 ng/mL in the rabbit reticulocyte-based in vitro translation assay (Table 2).

Effect of Mutations on the Cytotoxic Activity of Restrictocin. HeLa cells were permeabilized by infection with adenovirus and treated with restrictocin and its mutants to evaluate their cytotoxic activity. The incorporation of [^{3}H]-leucine in newly synthesized proteins was assayed, and the amount of toxin causing 50% inhibition was termed the ID_{50}. While restrictocin caused a dose-dependent inhibition of protein synthesis in the permeabilized HeLa cells with an ID_{50} value of 0.17 μg/mL, mutants Y47A, H49A, R120A, H136A, Y47A/H136A, and H49A/H136A were completely inactive and did not produce any inhibition of protein synthesis up to 100 μg/mL (Table 3). There was a dose-dependent protein synthesis inhibition by the E95A mutant; however, while restrictocin had an ID_{50} value of 0.17 μg/mL, E95A inhibited the protein synthesis with a much higher ID_{50} of 54 μg/mL (Table 3). Both F96A and P97A mutants were also cytotoxic to HeLa cells in a dose-dependent manner; however, they were found to have ~20-fold lower activity than restrictocin (Table 3).

Ribonucleolytic Activity of Restrictocin and Its Mutants. Rabbit reticulocyte lysate was treated at pH 7.5 with the native toxin and various mutants, and the total RNA was analyzed on a gel to detect the production of the 400-nucleotide α-fragment from the 28S rRNA (Figure 3A). In the ribonucleolytic activity assay, while restrictocin produced the characteristic α-fragment starting at 5 μg/mL, mutants R120A and H136A had no ribonucleolytic activity on the 28S rRNA (Figure 3A). There was no production of the α-fragment or the 5′ fragment from 28S rRNA with R120A

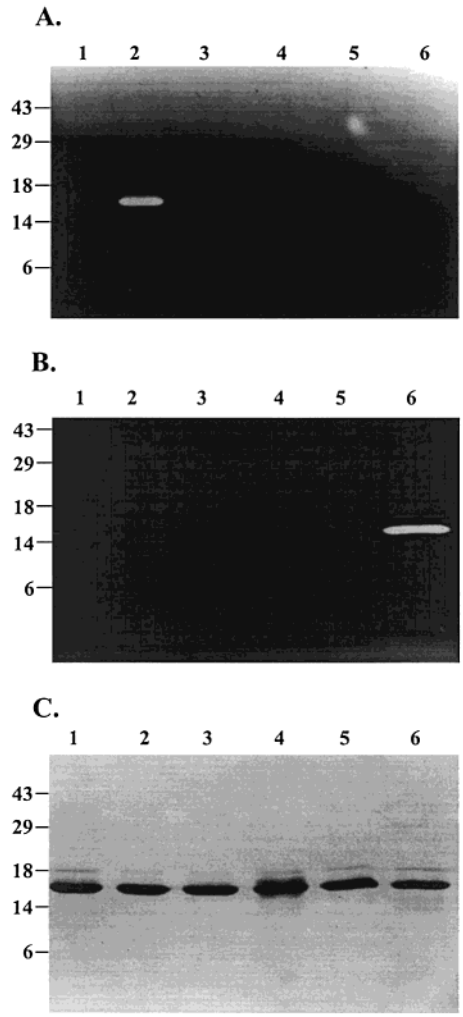

FIGURE 4: Zymogram electrophoresis of restrictocin and its mutants. Various proteins were subjected to SDS−PAGE under nonreducing conditions on 15% gels containing (A) poly(U), (B) poly(I), and (C) none. For gels in panels A and B, 250 ng of protein/lane was loaded, whereas for the gel shown in panel B, 2 μg of protein/lane was loaded. After removal of SDS, gels shown in panels A and B were stained with toluidine blue as described in Experimental Procedures. The gel shown in panel C was stained with Coomassie blue: lane 1, Y47A; lane 2, H49A; lane 3, H136A; lane 4, Y47A/H136A; lane 5, H49A/H136A; and lane 6, restrictocin.

and H136A even at 165 and 200 μg/mL, respectively, implying that Arg120 and His136 play a crucial role in restrictocin catalysis and are indispensable for the activity of the toxin (Figure 3A). All other Arg120 and His136 mutants, like R120A and H136A, failed to produce the typical α-fragment from the 28S rRNA up to 200 μg/mL (data not shown).

At low concentrations, mutants Y47A and H49A had no ribonucleolytic activity; however, with increasing concentrations, nonspecific degradation of the 28S rRNA was observed (Figure 3B). Mutants Y47A and H49A failed to recognize and cleave the target phosphodiester bond in the 28S rRNA to produce the characteristic α-fragment and instead digested the RNA nonspecifically.

With E95A, only a faint α-fragment band was visible at higher concentrations of the protein, indicating at least a partial but significant inactivation of the toxin as a result of mutation (Figure 3C). Mutants F96A and P97A produced the α-fragment as well as the larger fragment from the 5′

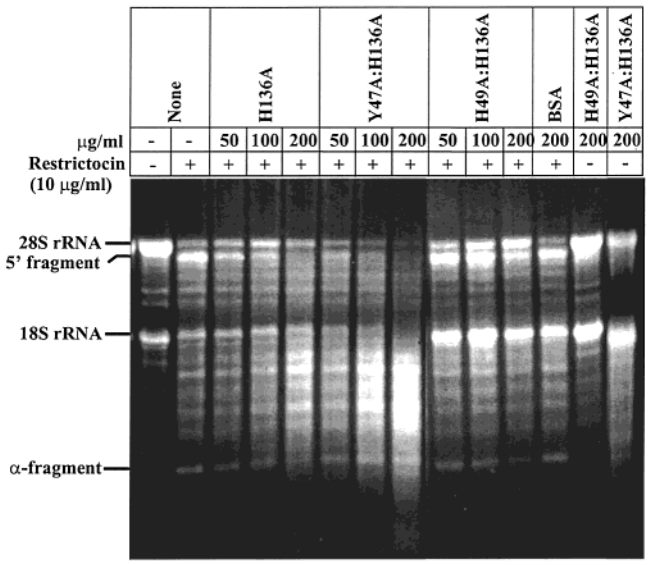

FIGURE 5: Effect of Y47A/H136A and H49A/H136A on the ribonucleolytic activity of restrictocin. Rabbit reticulocyte lysate was preincubated with various concentrations of the H136A, H49A/H136A, or Y47A/H136A mutant or BSA for 30 min on ice, followed by the addition of 10 μg/mL restrictocin. The mixture was incubated at 37 °C for 15 min, and the generation of the α-fragment was visualized on an agarose gel.

end of the 28S rRNA, whose intensity increased with increasing concentrations of the mutant, as for restrictocin (Figure 3C). Thus, mutation of Phe96 and Pro97 did not have any effect on the ribonucleolytic activity of the toxin.

Similar results were obtained with restrictocin and its mutants when the specific ribonucleolytic activity was determined at pH 5.5 (data not shown).

A zymogram electrophoresis assay was used to detect any contaminating ribonucleases in the protein preparations. As shown in Figure 4A, with the poly(U) substrate, a clear band was visible only with the H49A mutant in the region corresponding to its molecular weight, whereas with the poly(I) substrate, RNase activity was observed only with restrictocin (Figure 4B). Figure 4C shows various proteins run under nonreducing conditions on an SDS gel stained with Coomassie blue.

Role of Tyr47 and His49 in the Specificity of Restrictocin. To further investigate the roles of Tyr47 and His49, the specific ribonucleolytic activity of restrictocin was assayed separately in the presence of inactive mutants H136A, H49A/H136A, and Y47A/H136A. Mutant H136A competed with restrictocin, and in its presence, a decrease in the amount of the α-fragment as well as the 5′ fragment was observed (Figure 5). However, in the presence of mutants H49A/H136A and Y47A/H136A, there was no significant reduction in the level of generation of either the α-fragment or the 5′ fragment (Figure 5). BSA, used as a nonspecific control, produced no change in the activity of restrictocin in these assays (Figure 5). H49A/H136A and Y47A/H136A did not produce the α-fragment at the concentration used for the competition experiment (Figure 5). These results clearly demonstrate that the mutation of Tyr47 or His49 results in the loss of target recognition and/or binding ability of restrictocin.

Restrictocin−Substrate Model. We have analyzed a model of the restrictocin−29-mer RNA substrate complex (Figure

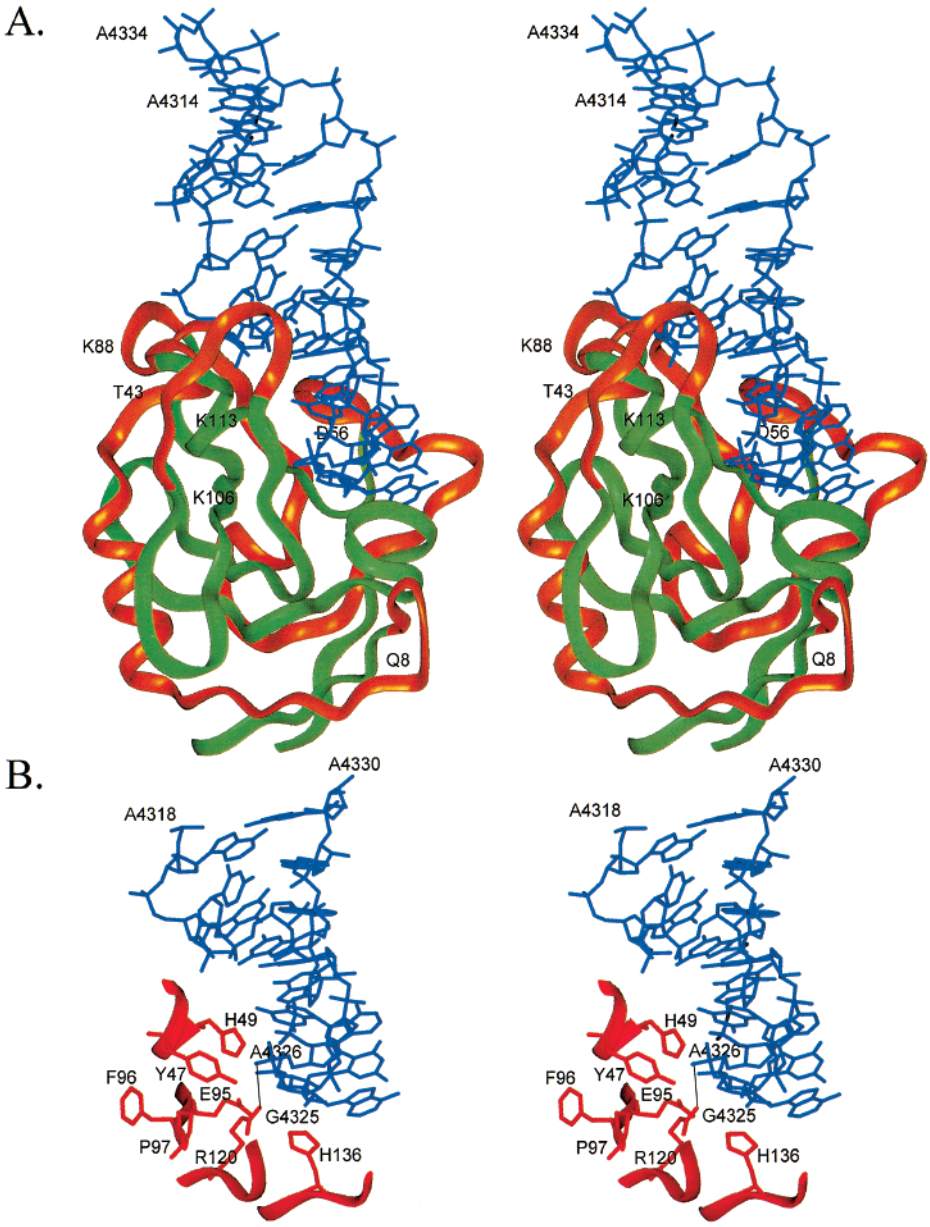

FIGURE 6: Model of the restrictocin−29-mer substrate analogue complex. (A) Stereodrawing of the complete molecular complex, where the ribbon represents restrictocin and the blue stick model corresponds to the RNA. The regions corresponding to the deletions made in mitogillin are shown in orange (*37*), while the rest of the protein is shown in green. The terminal residues of the deletion segments in the case of restrictocin are labeled. The RNA substrate region (A4314−A4334) is shown. (B) Stereodrawing of the active site region of the restrictocin−substrate complex. The side chains of residues Tyr47, His49, Glu95, Phe96, Pro97, Arg120, and His136 are explicitly highlighted as red sticks. The thin line represents the salt bridge between the cleavage site phosphate and the Arg120 side chain. The RNA substrate segment (A4318−A4330) is shown, and the nucleotides defining the cleavage site are labeled.

6) to provide further insight into the role of Tyr47, His49, Glu95, Phe96, Pro97, Arg120, and His136, the residues which were subjected to site-directed mutagenesis, in restrictocin catalysis. Our model of the RNA−restrictocin complex differs from that proposed previously (*11*) for two distinct reasons. First, the preliminary model presented by Yang and Moffat (*11*) used the NMR-derived RNA structure, whereas the structure of RNA used in the study presented here was determined by X-ray diffraction. Second, both the restrictocin and the substrate were held rigid in the previous docking studies (*11*), but in the study presented here, both RNA and the protein have been allowed conformational flexibility during MD simulation. The flexibility allowed in the protein and rRNA conformation led to significant optimization in the protein−nucleic acid interaction. The conformation showing a maximum intermolecular energy was compared to the native restrictocin and rRNA crystal structures. Between the bound and free restrictocin, there is a root-mean-square deviation of 1.94 and 3.31 Å in the position of the Cα atoms and all atoms, respectively. The lysine-rich loop of residues 106−116 moves significantly (root-mean-square deviation of 4.7 Å for the positions of all atoms when compared with those of native restrictocin) outward from the substrate-binding pocket compared with the native restrictocin structure. The interaction of residues of this loop with the rRNA molecule contributes −56.32 kcal/mol to the total intermolecular energy between rRNA and the substrate. The loop of residues 79−91 moves sideways (root-mean-square deviation of 3.5 Å) and contributes −12 kcal/mol, whereas the loop of residues 134−146 (root-mean-

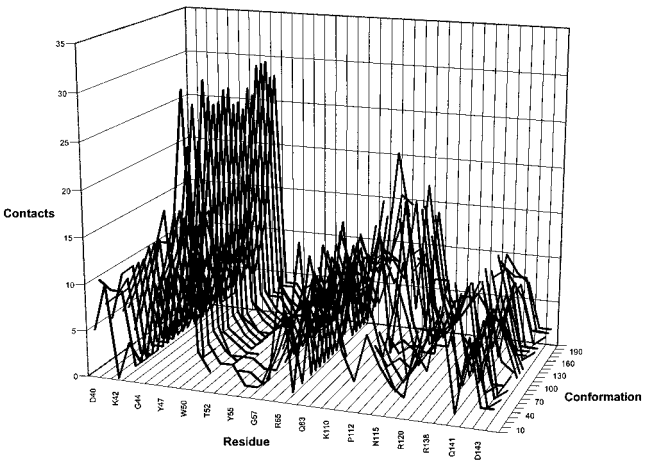

FIGURE 7: Comparison of restrictocin−substrate interaction during molecular dynamic simulation. The number of interactions formed by the residues of restrictocin with the rRNA substrate in different conformations recorded during the MD simulation is shown.

square deviation of 2.3 Å) moves inward to optimize the stability of the complex and contributes −42.2 kcal/mol to the total intermolecular energy. The loop of residues 53−67 also moves outward (root-mean-square deviation of 2.8 Å) to accommodate the substrate and contributes −21 kcal/mol to the intermolecular energy. The root-mean-square deviation in the position of all atoms for the rRNA molecule between the native and bound states is 1.2 Å.

The side chains of residues Phe96 and Pro97 are buried inside the protein and do not make any contact with the substrate. The phosphodiester bond between nucleotides G16 and A17 on the rRNA molecule which is the site of cleavage comes close to mutated residues Tyr47, His49, Glu95, Arg120, and His136 of restrictocin (Figure 6B). His49 forms a large number of contacts with nucleotides G14, G16, and A17. Tyr47 is present, adjacent to the cleavage site, and shows interactions with A17 and G16, and its hydroxyl group is present close to the phosphate of A17. Glu95 shows a number of interactions, most of which are with G16. Arg120 is also present close to the cleavage site and shows interactions with G16 and A17. A salt bridge is formed between the guanidinium group of Arg120 and the phosphodiester bond between G16 and A17 (which is the cleavage site). His136 shows a number of interactions with nucleotide G16. The base G10, analogous to G4319 of 28S rRNA, considered to be an identity element for ribotoxin recognition, and the cleavage site (the phosphodiester bond between G16 and G17) are on the same side of the RNA molecule and almost in line with each other. Nucleotide G10 forms a large number of contacts (both van der Waals and hydrogen bonding), most of which are with the Lys42, Ser46, Lys110, and Lys111 residues of the enzyme.

To identify residues, other than those that have been mutated, which might have a role in stabilizing the substrate onto the enzyme, the contacts between rRNA and the enzyme for all the conformations were compared. This comparison is shown graphically in Figure 7. It was seen that the residues Lys42, Trp50, Arg65, Gln83, Lys110, Lys111, and Lys113 consistently show a high number of contacts (which include van der Waals and hydrogen bonding interactions) with the rRNA molecule.

DISCUSSION

Restrictocin and the other members of the fungal ribotoxin family, α-sarcin and mitogillin, have a unique ability to specifically recognize and cleave a single phosphodiester bond in a GAGA tetranucleotide located in a conserved stem and loop structure termed the sarcin domain in the large ribosomal RNA. On the basis of the studies of other enzymes of this family and on the basis of the model of the restrictocin−RNA complex, many residues with a plausible functional role could be predicted. In this study, we have experimentally investigated the roles of Tyr47, His49, Glu95, Phe96, Pro97, Arg120, and His136, the amino acid residues forming the putative active site of restrictocin in its catalysis (*11*, *12*). Any mutation of Arg120 or His136 caused complete inactivation of restrictocin, while mutating Glu95 to Ala rendered the toxin partially inactive. In these mutants, the enzyme structure is unaffected. In the structural model of the substrate−enzyme complex, the cleavage site on the rRNA molecule comes close to residues Tyr47, His49, Glu95, Arg120, and His136 of restrictocin, showing direct contacts with the substrate.

Mutation of Tyr47 and His49 to Ala did not affect the hydrolysis of the RNA substrate, but the mutants failed to recognize the specific target. The restrictocin variants lacking either of the two residues caused nonspecific degradation of the target RNA instead of producing the typical α-fragment. In the case of the Tyr47Ala mutant, a change in the CD profile was observed, implying change in the structure of the protein; however, in the case of the His49Ala mutant, the loss in substrate specificity was not accompanied by any structural change in the protein. In a competition assay, double mutants H49A/H136A and Y47A/H136A failed to compete with native restrictocin and did not produce any change in the generation of the α-fragment from 28S rRNA, while the mutant H136A was able to compete and produced a decrease in the activity of the toxin. Mutation of Phe96 and Pro97 did not affect either the activity or the structure of restrictocin, implying that the side chains of these amino acid residues are not involved in restrictocin function or stabilization of structure. In the docking model, it is clear that the residues Phe96 and Pro97 are not exposed to the surface and make no contacts with the substrate.

Restrictocin and the other members of ribotoxin family are considerably homologous to RNase U2 and RNase T1. The antiparallel β-sheet and an adjacent long α-helix form the structural core of restrictocin, which represents a common structural motif found in other ribonucleases, including RNase T1, Ms, Sa, and barnase. The main differences are located in the length of the N-terminal β-hairpin and the loops connecting the secondary structure elements which are generally much longer in restrictocin and adopt conformations different from those in RNase T1 (*11*). It is evident from the model that these loops provide critical constraints defining the shape of the active site and are therefore major structural determinants of restrictocin specificity (Figure 6). On the basis of the studies on RNase T1, the mechanism of catalysis in restrictocin is believed to follow a two-step reaction (*11*). The first step is the phosphoryl transfer, in which His49 and Glu95 act as a general base to abstract a proton from the 2′-hydroxyl of a ribose and His136 serves as the general acid to protonate the 5′-oxygen of the leaving

nucleotide. In the second step of the hydrolysis reaction, the roles of catalytic residues are reversed. His136 acts as a general base and activates a water molecule, while His49 and Glu95 donate a proton to the 2′-oxygen. The activated water molecule then attacks the phosphorus atom in the intermediate and forms the second product, 3′-phosphate (*11*). There has been a general disagreement about the precise role of the corresponding residues, namely, His40 and Glu58 in RNase T1, as well (*31*).

We have demonstrated, in this study as well as in an earlier study (*15*), that the His49Ala mutant of restrictocin is completely ribonucleolytically active on a variety of RNA substrates but unable to specifically recognize the target RNA. A similar observation has recently been reported for a H50Q mutant of α-sarcin (*32*). Therefore, it is now apparent that His49 is not involved in the mechanistic aspect of the enzymatic activity of restrictocin but only in restricting the specificity of restrictocin for its target in the ribosomal RNA (*15*). Glu95 is appropriately located in the active site such that it can interact with the substrate to participate in the catalytic mechanism (Figure 6). However, the Ala substitution in its place led to only partial loss of activity. There is no other acidic residue in the vicinity of the active site which could be considered to take the place of Glu95 in the E95A mutant. The mutation of the equivalent residue in α-sarcin to glutamine, however, leads to complete loss of activity (*32*). Glu95 appears to be directly involved in the catalytic activity, and the removal of the side chain may bring in a residue in the neighborhood, which retrieves the activity only partially. The substitution with glutamine, which is essentially a nonacidic amino acid structurally similar to glutamic acid, will not sterically allow space for any other residue to come in its place. In the current study, mutation of His136 to a variety of residues, differing in side chain and charge, resulted in the total inactivation of restrictocin, indicating His at 136 position is an absolute requirement for acid−base catalysis. These findings with respect to His136 having a direct role in restrictocin catalysis corroborate the earlier observations in restrictocin and other ribotoxins (*13*, *14*). We have found restrictocin to manifest specific ribonucleolytic activity on the target rRNA, at both acidic and neutral pH. For the acid−base hydrolysis mechanism of RNA, Glu95 and His136 appear to be operating as the general base and general acid, respectively, in restrictocin. Recently, on the basis of the high pK_a values of His50, Glu96, and His137, the Glu96−H137 pair has been proposed to be acting as the general base and general acid in α-sarcin (*32*, *33*). In the docking model, these two residues, Glu95 and His136, come close to the cleavage site and form a number of interactions with nucleotides G16 and A17.

The inactivation of restrictocin as a result of substitution of Arg120 with a variety of residues indicates the indispensable nature of this residue. The docking model shows that this residue is present close to the cleavage site and forms a substantial number of interactions with nucleotides G16 and A17. The interactions include a salt bridge formed between its guanidinium group and the phosphodiester bond between G16 and A17 (which is the site at which restrictocin cleaves the rRNA). It is possible that the positively charged guanidinium group of the Arg120 residue stabilizes the negative charge of the cyclic RNA intermediate formed during catalysis.

It is shown in this study that Tyr47 and His49 are not directly involved in the actual cleavage reaction, although they are located in the active site and also exhibit direct interactions with RNA (Figure 6). However, the mutation of each of these residues to alanine makes the enzyme less specific. In the native restrictocin, Tyr47 is primarily involved in the stabilization of the β-sheet that scaffolds the active site. Therefore, there is some loss of structural rigidity of the active site, as reflected in the CD data, resulting in the broadening of the specificity of the enzyme. The mutation of His49 to alanine shows no change in the structure, while a similar change in function was observed. The docking model shows that His49 forms a large number of interactions with different nucleotides of the substrate. Thus, this residue by forming many specific contacts with the substrate ensures that the rRNA substrate is docked onto the enzyme in such a way that the cleavage site is oriented in the vicinity of the catalytically important residues. The model of the complex also shows that the Tyr47 residue forms interactions with the cleavage site itself and would be important in holding the phosphodiester in place so that the catalytic residues can carry out the appropriate chemical transformations on it. This is consistent with the role of the equivalent residue, Tyr45, in the active site of RNase T1 in substrate binding (*34*, *35*). Mutations His49Ala and Tyr47Ala would lead to the loss of these specific amino acids and hence would lead to nonspecific activity as seen in the biochemical experiments.

The structural comparison of RNase T1 and U2 with restrictocin has provided a possible explanation for the unique substrate specificity of restrictocin. The active site pocket of restrictocin is constrained by the loops, which do not exist in RNase T1 and U2. Kao and Davies (*36*) have shown that the deletion of residues 106−113 in mitogillin results in the loss of its specific substrate recognition activity. The deletion of amino acids 77−83 or 106−113 in mitogillin has been found to result in a complete loss of activity. It is seen in the docking model that the residues of the corresponding loops in restrictocin (79−91 and 106−116) show a large number of interactions with the rRNA substrate. Any mutations in these region would lead to loss of specific interactions and hence loss of the substrate specific recognition ability. Interestingly, deletions of regions within residues 1−25 show enhancement in the activity of the enzyme even though in the restrictocin−RNA complex model presented in the current study, this part does not appear to have any direct contacts with the RNA (*37*). However, the two strands of the β-sheet constituting these residues provide stabilizing support to the loop of residues 138−144, which has a critical role in defining the active site cleft. In the model of the complex, this loop shows a very large number of interactions with the rRNA substrate and contributes substantially to the intermolecular energy between the enzyme and substrate. Apparently, deletions in the first 25-residue stretch make the loop of residues 138−144 flexible enough to reduce the strains on the active site (*37*). The deletion of Lys28−Ser31, which includes the α-helix, may be disturbing the entire protein structure, resulting in the complete inactivation of mitogillin (*37*). The deletion analysis of related substrate specific RNases and the model of the restrictocin−substrate complex provide support to the hypothesis that the substrate specificity shown by these RNases against others is due to the loops present around the active site.

In conclusion, the study presented here provides functional and structural delineation of the restrictocin active site. It is evident that certain residues directly contribute to the enzyme catalysis, others provide structural stability to the active site, and still others determine the substrate specificity of the enzyme. On the basis of their functions, the putative active site residues could be classified under four categories. (i) Tyr47 and His49 are involved in the recognition of the target RNA by the toxin. (ii) Arg120 could be anchoring the substrate in place in the active site. (iii) His136 and Glu95 appear to be directly involved in the acid−base mechanism of RNA hydrolysis by restrictocin. (iv) Phe96 and Pro97 are not involved in the catalytic activity of restrictocin.

REFERENCES

1. Lopez-Otin, C., Barber, D., Fernandez-Luna, J. L., Soriano, F., and Mendez, E. (1984) *Eur. J. Biochem. 143*, 621−634.
2. Lamy, B., Davies, J., and Schindler, D. (1992) in *Genetically Engineered Toxins* (Frankel, R. E., Ed.) pp 237−258, Marcel Dekker, New York.
3. Schindler, D. G., and Davies, J. E. (1977) *Nucleic Acids Res. 4*, 1097−1110.
4. Endo, Y., and Wool, I. G. (1982) *J. Biol. Chem. 257*, 9054−9060.
5. Chan, Y.-L., Endo, Y., and Wool, I. G. (1983) *J. Biol. Chem. 258*, 12768−12770.
6. Fernandez-Puentes, C., and Vazquez, D. (1977) *FEBS Lett. 78*, 143−146.
7. Endo, Y., Chan, Y.-L., Lin, A., Tsurugi, K., and Wool, I. G. (1988) *J. Biol. Chem. 263*, 7917−7920.
8. Endo, Y., Gluck, A., Chan, Y.-L., Tsurugi, K., and Wool, I. G. (1990) *J. Biol. Chem. 265*, 2216−2222.
9. Gluck, A., and Wool, I. G. (1996) *J. Mol. Biol. 256*, 838−848.
10. Correll, C. C., Munishkin, A., Chan, Y.-L., Ren, Z., Wool, I. G., and Steitz, T. A. (1998) *Proc. Natl. Acad. Sci. U.S.A. 95*, 13436−13441.
11. Yang, X., and Moffat, K. (1996) *Structure 4*, 837−852.
12. Martinez Del Pozo, A., Gasset, M., Onaderra, M., and Gavilanes, J. G. (1988) *Biochim. Biophys. Acta 953*, 280−288.
13. Yang, R., and Kenealy, W. R. (1992) *J. Biol. Chem. 267*, 16801−16805.
14. Lacadena, J., Mancheno, J. M., Martinez-Ruiz, A., Martinez Del Pozo, A., Gasset, M., Onaderra, M., and Gavilanes, J. G. (1995) *Biochem. J. 309*, 581−586.
15. Nayak, S. K., and Batra, J. K. (1997) *Biochemistry 36*, 13693−13699.
16. Kao, R., Shea, J. E., Davies, J., and Holden, D. W. (1998) *Mol. Microbiol. 29*, 1019−1027.
17. Nayak, S. K., Rathore, D., and Batra, J. K. (1999) *Biochemistry 38*, 10052−10058.
18. Rathore, D., and Batra, J. K. (1996) *Biochem. Biophys. Res. Commun. 222*, 58−63.
19. Rathore, D., and Batra, J. K. (1997) *Biochem. J. 324*, 815−822.
20. Rathore, D., and Batra, J. K. (1997) *FEBS Lett. 407*, 275−279.
21. Goyal, A., and Batra, J. K. (2000) *Biochem. J. 345*, 247−254.
22. Rathore, D., Nayak, S. K., and Batra, J. K. (1996) *FEBS Lett. 392*, 259−262.
23. Kunkel, T. A., Roberts, J. D., and Zakour, R. A. (1987) *Methods Enzymol. 154*, 367−382.
24. Sanger, F., Niklen, S., and Coulson, A. R. (1977) *Proc. Natl. Acad. Sci. U.S.A. 74*, 5463−5467.
25. Buchner, J., Pastan, I., and Brinkmann, U. (1992) *Anal. Biochem. 205*, 263−270.
26. Bal, H. P., and Batra, J. K. (1997) *Eur. J. Biochem. 245*, 465−469.
27. Fernandez-Puentes, C., and Carrasco, L. (1980) *Cell 20*, 769−775.
28. Nayak, S. K., Bagga, S., and Batra, J. K. (2000) *Eur. J. Biochem. 267*, 1777−1783.
29. Lacadena, J., Martinez Del Pozo, A., Barbeto, J. L., Mancheno, J. M., Gasset, M., Onaderra, M., Lopez-Otin, C., Ortega, S., Gracia, J., and Gavilanes, J. G. (1994) *Gene 142*, 147−151.
30. Blank, A., Sugiyama, R. H., and Dekker, C. A. (1982) *Anal. Biochem. 120*, 267−275.
31. Steyaert, J. (1997) *FEBS Lett. 247*, 1−11.
32. Lacadena, J., del Pozo, A. M., Ruiz-Martinez, A., Perez-Canadillas, J. M., Bruix, M., Mancheno, J. M., Onaderra, M., and Gavilanes, J. G. (1999) *Proteins: Struct., Funct., Genet. 37*, 474−484.
33. Perez-Canadillas, J. M., Campos-Olivas, R., Lacadena, J., del Pozo, A. M., Gavilanes, J. G., Santoro, J., Rico, M., and Bruix, M. (1998) *Biochemistry 37*, 15865−15876.
34. Höschler, K., Hoier, H., Hubner, B., Saenger, W., Orth, P., and Hahn, U. (1999) *J. Mol. Biol. 294*, 1231−1238.
35. Hubner, B., Haensler, M., and Hahn, U. (1999) *Biochemistry 38*, 1371−1376.
36. Kao, R., and Davies, J. (1995) *Biochem. Cell Biol. 73*, 1151−1159.
37. Kao, R., and Davies, J. (1999) *J. Biol. Chem. 274*, 12576−12582.

BI010923M